

## Generation of plasma flows by arc plasmatrons

A S Anshakov<sup>1</sup>, P V Domarov<sup>2</sup>, V A Faleev<sup>1</sup>, A A Danilenko<sup>2</sup>

<sup>1</sup>Kutateladze institute of thermophysics SB RAS, Lavrentiev av. 1, Novosibirsk, 630090, Russia

<sup>2</sup>Novosibirsk State Technical University, Karl Marx av. 20, Novosibirsk, 630073, Russia

E-mail: anshakov@itp.nsc.ru

**Abstract.** Plasma technologies of material modification and deposition of coatings with different functional properties can be implemented if the efficient sources of plasma flows are available. These sources are the electric-arc generators of thermal plasma (plasmatrons). The effect of different plasmatron schemes on distribution of temperature and velocity of plasma flows is considered in the current study. For example, it is shown that a partitioned interelectrode insert and gas injection between the sections ensure a plateau in temperature distribution  $T(r)$ . A similar result was obtained for the plasma flow at the exit of the plasmatron with a stepped output electrode.

### 1. Introduction

Despite the variety of designs of electric-arc plasma generators, they are divided into two types. The first type includes the jet plasmatrons, and the second one joins the melting plasmatrons. In this paper, we will focus on the jet plasmatrons, designed for surface treatment of products. The latter includes many processes, such as deposition of powder materials of various functional purposes, hardening the surfaces of machine mechanisms, modification of surfaces of the metal and non-metal products, etc.

Each of these and other processes requires high-performance long-life electric-arc plasmatrons, meeting the requirements of a particular technology. To implement any process, a set of certain plasmatron parameters and characteristics, making it possible to achieve the required quality, performance, repeatability, and cost-effectiveness, is required. For this reason, various design schemes of plasmatrons, which can ensure full implementation of the specified process parameters through the use of plasma flows with their individual characteristics on temperature and velocity distribution, are being developed.

### 2. Features of plasma flows for different plasmatrons

#### 2.1. Plasmatron with partitioned interelectrode insert (IEI).

The plasmatron scheme is shown in Fig. 1 [1]. The interelectrode insert (IEI) is designed to obtain a higher voltage on the arc than that in other plasmatron constructions. To reduce heat losses in discharge chamber walls, cold gas injection  $g_i$  between the sections is used.



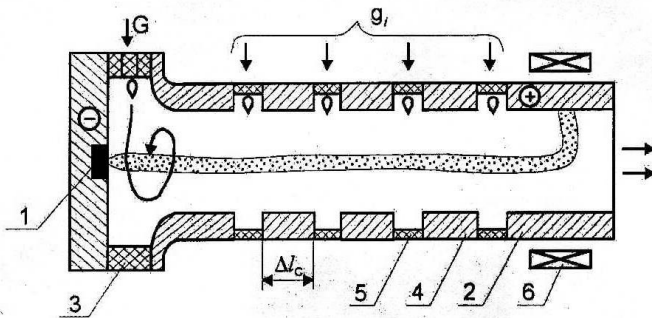


**Figure 1.** Plasmatron with interelectrode insert (IEI): 1 – cathode, 2 – anode, 3 – unit of main gas flow  $G$  input, 4 – IEI section, 5 – unit of intersectional gas flow  $g_i$  input, 6 – solenoid.

We will present the experimental data on the study of the plasma flow temperature field for the plasmatron with IEI. The plasmatron power versus arc current is 150-350 kW. The diameter of sections is  $10 \cdot 10^{-3}$  m, the diameter of output electrode is  $d_A = 14 \cdot 10^{-3}$  m, and IEI length is  $a = 0.3$  and  $0.4$  m. The total air flow rate is  $G = 10 \cdot 10^{-3}$  kg/s,  $g_i = 0.3 \cdot 10^{-3}$  kg/s. The jet temperature was measured by the method of relative intensities of the spectral lines of copper CuI 5105.5 nm and CuI 5153.2 nm by a quartz spectrograph ISP-28. Local thermal equilibrium in the plasma jet was assumed. Radial temperature distributions in the plasma air jet at different arc currents, measured at distance  $z = 1 \cdot 10^{-2}$  m from the nozzle edge, indicate constant temperature along the jet radius with the coefficient of profile flattening from 40% at  $I = 70$  A to 95% at  $I = 180$  A.

The plateaus in the radial distribution of jet temperature are caused by intense turbulent mixing of cold gas, supplied uniformly along the channel length, with gas heated in the arc chamber. In addition, a step in the channel, formed by a sharp transition from IEI diameter to the diameter of the output electrode, also facilitates the alignment of the profile of heated gas temperature at the plasmatron outlet.

The temperature field of the studied plasma jet, plotted by the results of 2-4 temperature measurements in different cross-sections is shown in Fig. 2. The type of radial temperature distributions with plateau  $T(r)$  is kept up to high values of  $z$ .

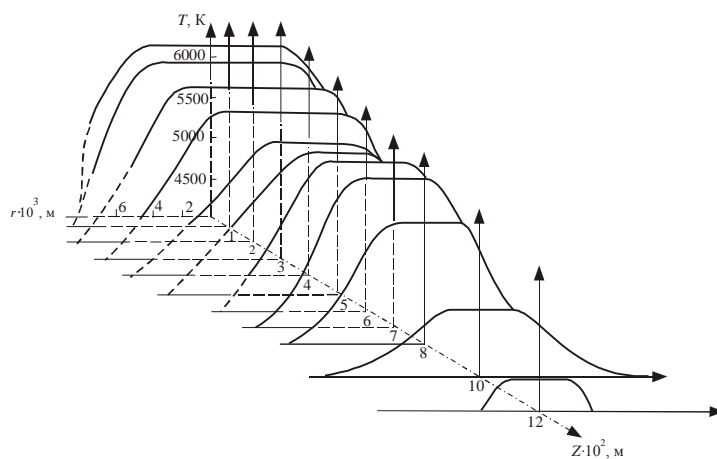


**Figure 2.** Temperature field of a plasma jet from the plasmatron with a partitioned IEI:  $d = 1 \cdot 10^{-2}$  m;  $\bar{a} = 30$ ;  $G = 10 \cdot 10^{-3}$  kg/s;  $I = 120$  A;  $d_A = 1,4 \cdot 10^{-2}$  m.

The curves in Fig. 2 indicate that up to  $z = (5-6) \cdot 10^{-2}$  m the temperature profile leveling decreases and then increases again. Moreover, in the zone of the mentioned cross-sections of the jet, the temperature at the axis increases slightly, and the temperature profile in the boundary layer changes (it becomes flatter). The experimental data allowed us to determine the border of a potential core (initial region of the jet) and zone of transition. In our case, the jet core extends to  $z = (7-8) \cdot 10^{-2}$  m. In the

initial region, the temperature along the jet decreases slowly (the axial temperature gradient is about 50 C/cm) and its drop is determined by energy removal through radiation. Starting from cross-section  $z = 8 \cdot 10^{-2}$  m, the temperature along the jet axis decreases significantly faster (the axial temperature gradient is 300 C/cm).

To explain the features of radial temperature distributions along the jet, the studied jet was recorded by a high-speed camera SKS-1M. The sequences of frames demonstrate that the end of the high-temperature core is subjected to spiral rotation, caused by residual swirl of stabilizing gas. It leads to more intense mixing of the boundary layer with the high-speed potential core, intensifying boundary layer removal in this area, which, in turn, causes cold gas inflow from the periphery and, as a sequence, temperature reduction in the considered region ( $z = (4-6) \cdot 10^{-2}$  m in Fig. 2).

### 2.2. Plasmatron for deposition of powder coatings.

Plasma deposition of powder materials on the components and products is a common electro-technological process in mechanical engineering, power engineering, electronics, aviation and space technologies. The technology is very effective for deposition of many types of protective coatings. The sources of high-speed and high-temperature flows for powder spraying are the compact electric-arc plasmatrons with the power from 10 to 50 kW. The plasmatrons with partitioned IEI and fixed average arc length are the most common. The plasma-forming gases are: argon, nitrogen, natural gas, air, and mixtures thereof.

The principle scheme of a plasmatron with IEI is shown in Fig. 3. The arc discharge length is determined by the length of IEI. Nitrogen flow rate is  $G_1 = 0.8 \cdot 10^{-3}$  kg/s, argon flow rate is  $G_2 = 0.2 \cdot 10^{-3}$  kg/s.

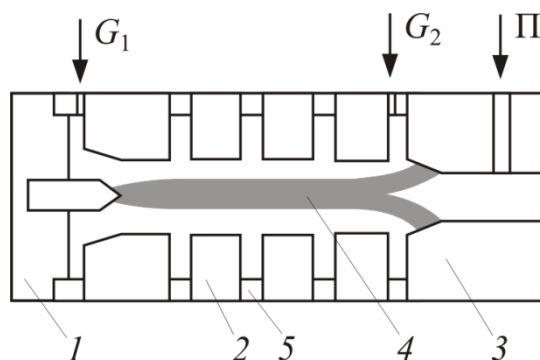


**Figure 3.** Plasmatron with IEI for spraying:  
1 – cathode, 2 – IEI section, 3 – anode, 4 – electric arc, 5 – inter-sectional insulators,  $\Pi$  – point of powder input.

The linear circuit plasmatrons for spraying differ from those with gas-vortex arc stabilization by the absence of swirl gas flow in the discharge chamber. This is caused by transverse dispersion of powder, introduced into the jet at the plasmatron outlet due to exposure of particles to the centrifugal forces. Therefore, axial supply of the working gas is mainly used in the spraying plasmatrons or specific measures are taken to eliminate the circumferential component of the jet velocity.

Comparative data on the plasma flow temperatures in the plasmatron with self-sustained arc length GN-5R (curves 1-3) and plasmatron with IEI (curve 4) are shown in Fig. 4 [2]. The efficiency of plasma-forming gas heating in the plasmatron with a fixed length is obvious.

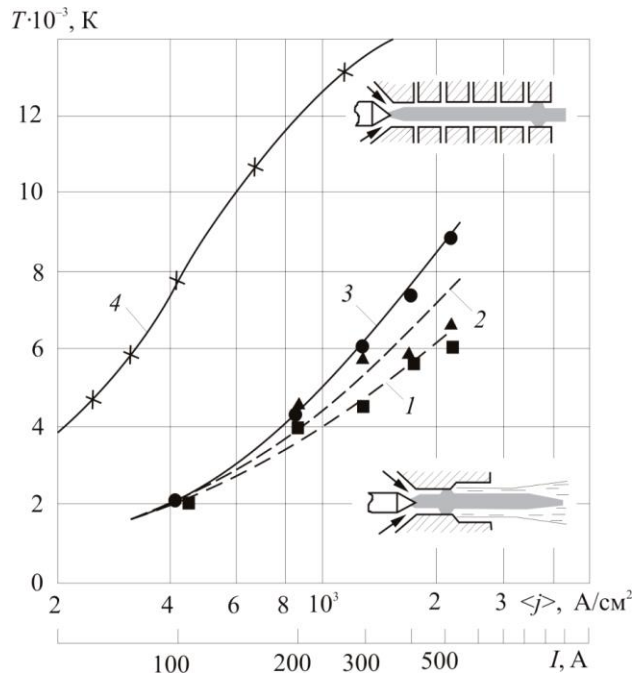


**Figure 4.** Mean mass temperature of the argon plasma jet for the plasmatron with IEI and GN-5R at the following gas flow rates,  $\times 10^{-3}$  kg/s: 1 – 0.39, 2 – 0.67, 3 – 1.23, 4 – 0.67.

Differences in the parameters and characteristics of discharge glow in plasmatrons with different arc lengths affect the characteristics of the effluent plasma jets, responsible for the properties of coatings: adhesion strength, density, structure, etc. The studies have shown that the shape and characteristics of the jet depend on location of the reference arc spot in the output electrode and have an asymmetrical form. When the anode spot goes to a new location due to the processes of arc bridging, gas flow pulsations or other reasons, the jet parameters at the point of powder supply change and it affects the quality and repeatability of the process. In a partitioned plasmatron, the jet is symmetrical and more compact. Consequently, the angle of jet opening with the powder is smaller than that of the plasmatron with the tubular or stepped output electrode. Accordingly, the use factor of powder and coatings quality increase.

The plasma jet parameters were studied experimentally on the plasmatron with the interelectrode insert EDP-167, developed at the Institute of Thermophysics SB RAS (diameter of IEI sections is  $8 \cdot 10^{-3}$  m, IEI length is  $60 \cdot 10^{-3}$  m, and diameter of the anode nozzle is  $6 \cdot 10^{-3}$  m) using a water-cooled Gray probe. At that, time-averaged dynamic pressure  $\Delta p$  and enthalpy increment  $\Delta h$  were determined. The probe was moved along plasma jet axis  $z$  and its radius  $r$  using a coordinate device. Radial distributions of enthalpy and dynamic pressure near the nozzle have a sharp peak at the jet axis and with an increase in coordinate  $z$  these profiles flatten out noticeably. Distributions of  $\Delta p$  and  $\Delta h$  along the jet axis for argon and nitrogen-argon mixture are shown in Figs. 5 and 6.

It is evident that enthalpy at the argon jet within the acceleration area and powder particles heating is considerably lower than that of the nitrogen-argon jet. This result is a consequence of an increase in the plasmatron power with increasing percentage of nitrogen in the plasma-forming gas (at the constant arc current and gas flow rate, the transition from argon to nitrogen leads to an increase in discharge voltage more than twice).

### 2.3. Plasmatron with the stepped output electrode.

The simplest scheme of plasmatron is shown in Fig. 7 [1]. An abrupt channel expansion (step) generates the gas-dynamic conditions for predominant arc bridging just after the zone of flow detachment and ensures the constancy of its average length in a wide range of current strength, gas flow rate and pressure for constant  $l$  and  $d$ .

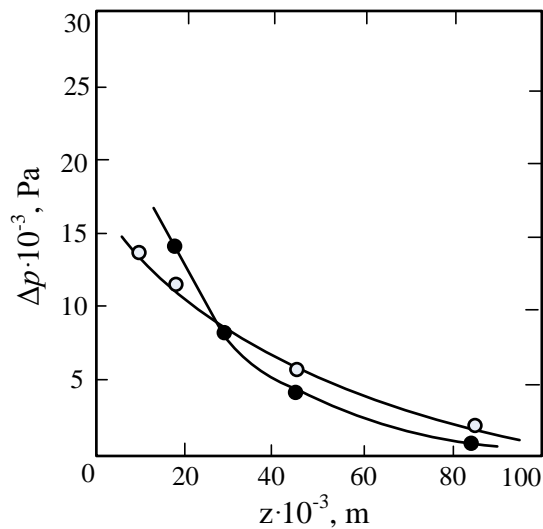


**Figure 5.** Distributions of dynamic pressure along the plasma jet.  $I = 100$  A,  $G = 1 \cdot 10^{-3}$  kg/s; o – Ar, ● – 80%  $N_2 + 20\%$ Ar.

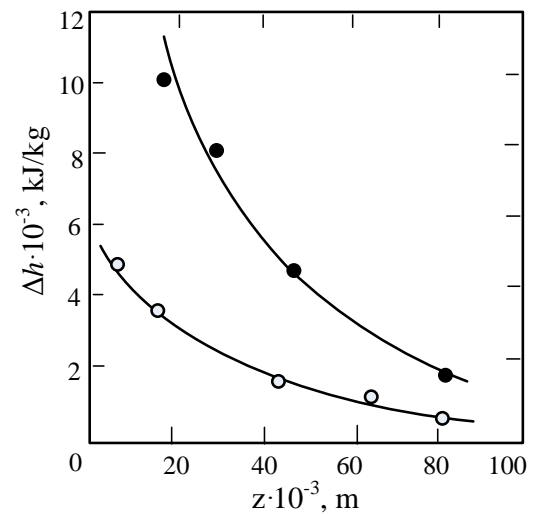


**Figure 6.** Distribution of enthalpy along the plasma jet.  $I = 100$  A,  $G = 1 \cdot 10^{-3}$  kg/s; o – Ar, ● – 80%  $N_2 + 20\%$ Ar.

According to spectral and pneumatic measurements [4], plateau  $T(r)$  in temperature distribution along the radius is observed with 10-% accuracy in the plasma jet core at the outlet of nozzle with diameter  $D$ . The profiles of plasma flow are uniform (Fig. 8), and this proves intensive mixing of the hot and cold gases at flow separation on a step in the output electrode.

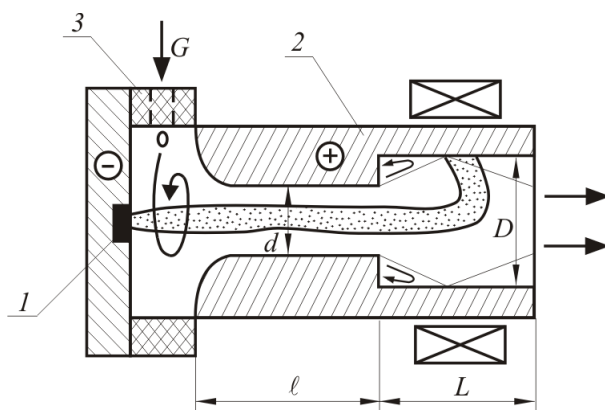


**Figure 7.** Scheme of plasmatron with fixation of the average arc length by a step: 1 – inner electrode; 2 – outer electrode of stepped geometry; 3 – vortex chamber for the gas input with flow rate  $G$ .

The plasma flows of the two-jet plasmatron are of a particular scientific and practical interest [1]. The arc discharge beyond the electrodes increases significantly the flow temperature of different plasma-forming media and opens a broad perspective of their practical application in the field of modifying the product surfaces.

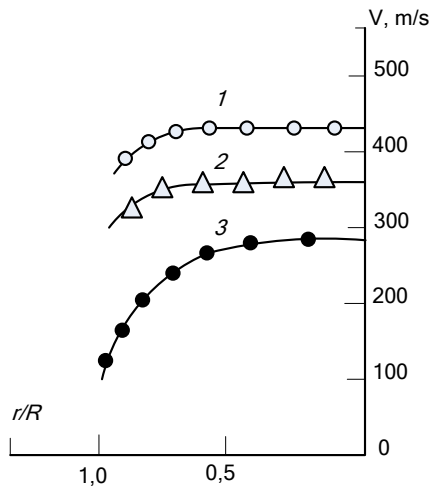


**Figure 8.** Radial distribution of plasma flow velocity.  $D = 40 \cdot 10^{-3}$  m,  $G = 40 \cdot 10^{-3}$  kg/s,  $I = 500$  A. Distance from the nozzle edge: 1 –  $z = 0.5D$ , 2 –  $z = D$ , 3 –  $z = 2D$ .

### 3. Conclusion

The interconnection of a plasmatron structural scheme with plasma flow parameters is shown. It was determined for different designs of jet plasmatrons that the plasma flow structure is determined by the flow of plasma-forming gas in the discharge chamber.

The investigation results are required not only for application to a specific technology, but also for understanding the physical processes of arc glow at forced heat exchange with the plasma-forming gas.

### References

- [1] Cherednichenko V S, Anshakov A S, Kuzmin M G 2011 *Plasma Electrotechnological Installations* (Novosibirsk: NSTU)
- [2] Donskoy A V, Klubnikin V S 1979 *Electroplasma Processes and Installations in Mechanical Engineering* (Leningrad: Mashinostroenie)
- [3] Timoshevskiy A N, Vasilkovskaya A S, Ginal S V 1977 *VII Proc. All-Russian Conf. on Generators of Low-Temperature Plasma* vol 1 (Alma-Ata: Energy Institute) pp 242–245

### Acknowledgments

This work was financially supported by the Russian Ministry of Education and Science, according to Subsidy Agreement No.14.607.21.0118 (unique project identifier RFMEF160715X0118).